Annales Geophysicae (2004) 22: 2797–2804
SRef-ID: 1432-0576/ag/2004-22-2797

Annales Geophysicae

Parallel electric field in the auroral ionosphere: excitation of acoustic waves by Alfvén waves

P. L. Israelevich[1] **and L. Ofman**[2]

[1]Department of Geophysics and Planetary Sciences, Raymond and Beverly Sackler Faculty of Exact Sciences, Tel Aviv University, Ramat Aviv, 69978, Israel
[2]Department of Physics, The Catholic University of America and NASA Goddard Space Flight Center, Code 682, Greenbelt, MD 20771, USA

Received: 27 August 2003 – Revised: 14 April 2004 – Accepted: 5 May 2004 – Published: 7 September 2004

Abstract. We investigate a new mechanism for the formation of a parallel electric field observed in the auroral ionosphere. For this purpose, the excitation of acoustic waves by propagating Alfvén waves was studied numerically. We find that the magnetic pressure perturbation due to finite amplitude Alfvén waves causes the perturbation of the plasma pressure that propagates in the form of acoustic waves, and gives rise to a parallel electric field. This mechanism explains the observations of the strong parallel electric field in the small-scale electromagnetic perturbations of the auroral ionosphere. For the cases when the parallel electric current in the small-scale auroral perturbations is so strong that the velocity of current carriers exceeds the threshold of the ion sound instability, the excited ion acoustic waves may account for the parallel electric fields as strong as tens of mV/m.

Key words. Ionosphere (Electric fields and currents; Plasma waves and instabilities; Polar ionosphere)

1 Introduction

One of the most important questions of the auroral physics is the origin of strong small-scale electric fields (transverse to the ambient magnetic field) and their relation to the auroral phenomena, in particular, to the parallel electric fields and particle acceleration. Since the existence of a strong localized electric field has been observed by S3-3 satellite (Mozer et al., 1977), numerous studies of spatial distribution of these events have established that small-scale strong transverse electric fields are common in the regions connected to the auroral zone up to the altitude of at least $20\,R_E$ (Mozer et al., 1980; Mizera et al., 1981; Temerin et al., 1981; Mozer, 1981; Cattell et al., 1982; Levin et al., 1983; Bennett et al., 1983; Burke et al., 1983; Gurnett et al., 1984; Redsun et al., 1985; Lindqvist and Marklund, 1990; Weimer and Gurnett, 1993; Karlsson and Marklund, 1996). Moreover, there is evidence that the same phenomena are observed in the distant geomagnetotail (Cattell et al., 1994; Streed et al., 2001). The above observations show that significant parallel component of the electric field usually accompanies a strong transverse electric field. The existence of a parallel electric field was suggested long ago by McIlwain (1960), based on the spectra of precipitating electrons. Evidence of parallel fields was obtained by observation of upstreaming ion beams (Shelley et al., 1976).

The auroral electric field measured at different altitudes results from the electric field of the magnetospheric convection by mapping along almost equipotential magnetic field lines. Geometrical convergence of the magnetic field lines results in an increase of the transverse electric field on approach to Earth. The fact that the electric field at lower altitude is weaker than expected from simple geometrical consideration is interpreted as an evidence for a field-aligned electric potential drop (e.g. Mozer, 1981). However, the parallel electric field accompanying the mapping of the electrostatic structures is expected to be of the order of <1 mV/m, whereas the direct measurements of the parallel component of the electric field are indicative of larger values of tens mV/m (Mozer et al., 1977; Dubinin et al., 1985). Unfortunately, initial measurements of a strong parallel electric field were received skeptically by the scientific community and had small impact on the auroral research, perhaps due to the lack of theory explaining large values of the parallel electric fields.

Simultaneously with the development of electrostatic theory of the phenomenon, other theoretical studies suggested that at least some of the observed events can be caused by Alfvén waves having, therefore, an electromagnetic nature (Hasegawa, 1976; Malinckrodt and Carlson, 1978; Goertz and Boswell, 1979; Lysak and Dum, 1983; Haerendel, 1983; Goertz, 1984; Glassmeier et al., 1984). This point of view found experimental support in the results of Intercosmos-Bulgaria-1300 satellite, which performed simultaneous measurements of electric and magnetic fields along with plasma

Correspondence to: P. L. Israelevich
(peter@luna.tau.ac.il)

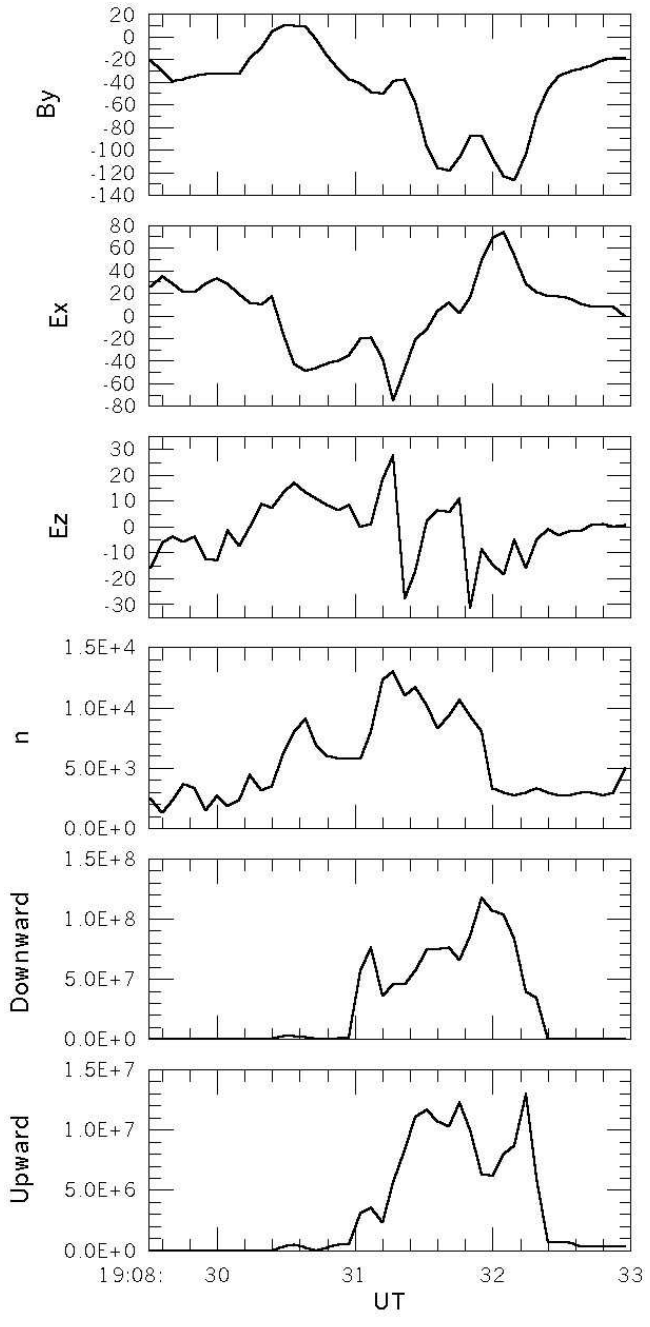

Fig. 1. An example of auroral electromagnetic perturbation observed by the Intercosmos-Bulgaria-1300 satellite. From top to bottom: transverse magnetic field B_y and electric field E_y perturbations, parallel electric field E_z, number density n, and downward and upward fluxes of electrons with the energy 1 keV.

and energetic particles (Dubinin et al., 1985, 1990). Alfvén waves were also observed during the rocket experiments at regions of auroral arcs (Gelpi and Bering, 1984). Recently, a case study by Wygant et al. (2000) confirmed that some electric field structures seen in the auroral zone and above could be caused by Alfvén waves.

The transverse component of the wave vector in small scale Alfvénic perturbations is much larger than the parallel component $k_\perp \gg k_{||}$. For the cases where $k_\perp \lambda_e = k_\perp c/\omega_0 \geq 1$ (where λ_e is the electron inertial length, and ω_0 is the plasma frequency), the wave becomes an inertial Alfvén wave and carries parallel electric field $E_{||} \sim E_\perp k_{||}/k_\perp$. In principle, this parallel electric field component may account for the particle acceleration in the small-scale electromagnetic structures.

Another approach to explain the existence of parallel electric fields combines electromagnetic and anomalous resistivity effects (e.g. Lysak and Carlson (1981); Lysak and Dum (1983); Volokitin et al. (1983); Streltsov et al. (2002)). Dubinin et al. (1984) have tried to relate an intense localized disturbance with processes of Alfvén wave propagation and plasma turbulence excitation within auroral flux tube. However, even in the framework of such models, it is difficult to understand the existence of cavities of the ion density (Dubinin et al., 1985), large (tens of mV/m) field-aligned electric fields, and phase relations between electric and magnetic fields.

Some phenomena of electrostatic nature are closely related with the small-scale Alfvén waves and have been studied intensively. For example, electrostatic convective cells may form with spatial scales larger than the scale of the Alfvén wave. Pokhotelov et al. (2003) suggested parametric instability of the initial inertial Alfvén wave as a mechanism responsible for the convection cells formation. Another, possibility for small-scale electromagnetic perturbation is often associated with waves at hydrogen and oxygen local gyrofrequencies (e.g. Kintner, 1980; Andre et al., 1987; Cattell et al., 1998). These waves are interpreted as electrostatic ion cyclotron (EIC) waves due to the instability of the particle beams (Kindel and Kennel, 1971)

However, electromagnetic models of small-scale auroral structures still contain difficulties with the explanation of observations, and with the understanding of the nature of strong parallel electric fields.

Figure 1 shows an example of localized electromagnetic perturbation in the auroral ionosphere as observed on the Intercosmos-Bulgaria-1300 satellite at the altitude of 900 km in the morning sector within the region of a large-scale downward field-aligned electric current. Such a pattern is typical for the observations of strong small-scale auroral electromagnetic perturbation at these altitudes. From top to bottom we show the X- and Y-components of the magnetic field perturbation, X-, Y-, and Z-components of the electric field, plasma density and upward and downward fluxes of 1-keV electrons. (The Z axis is directed along the ambient magnetic field and is close to the local vertical.) The transverse (to the ambient magnetic field) component of the electric field is predominantly in the X direction, and the transverse component of the magnetic field perturbation is predominantly in the Y direction. The ratio of amplitudes of E_x to ΔB_y equals to local Alfvén velocity, as expected for the electromagnetic wave. Both E_x and ΔB_y have similar spectra, but the magnetic field harmonics are shifted by $\pi/2$ with respect to the electric field harmonics. This phase relation

is rather typical for the small-scale electromagnetic auroral perturbations (Streltsov and Lotko, 2003; Streltsov and Mishin, 2003; Mishin et al., 2003). Using this phase relation, Dubinin et al. (1985, 1990) interpreted the perturbation as a standing monochromatic Alfvén wave and separated temporal and spatial effects in the observations. The separation results in the frequency of the wave $f \approx 1$ Hz, and transverse and parallel wave vector components $k_\perp \approx 7\times10^{-6}$ cm^{-1} and $k_{||} \approx 3.5\times10^{-8}$ cm^{-1}, respectively. The local electron inertia length is $\lambda_e \approx 5\times10^3$ cm, thus, at least at these altitudes, $k_\perp \lambda_e \ll 1$ and the electron inertia can be neglected.

However, a standing localized Alfvén wave does not explain the variations of density and the presence of a strong (up to 30 mV/m) parallel electric field (see panels (e) and (f) in Fig. 1). The number density and E_z oscillate with the frequency twice larger than that of the standing Alfvén wave responsible for the E_x and ΔB_y components ($\approx$2 Hz). Strong perturbation of the parallel electric field E_z is of an electrostatic nature, since no perturbation at the same frequency is observed in the magnetic field.

The perturbation is accompanied by a burst of energetic electrons. Upward and downward fluxes of electrons at 1 keV have the opposite phase which is indicative of particle flux modulation by alternating parallel electric field.

The observed E_z cannot be ascribed to the electrostatic ion cyclotron waves for the following reasons. First, the frequency of the local ion gyrofrequency is $\sim$470 Hz for H^+ and $\sim$30 Hz for O^+. Second, the EIC waves have been observed at local ion gyrofrequency by the satellites at different altitudes; e.g. S3-3 (Kintner 1980); Viking (Andre et al., 1987), and FAST (Cattell et al., 1998). This means that EIC waves are excited locally and do not propagate to large distances. Therefore, it is unlikely that the observed event is an EIC wave excited in the region with the local field $\sim$300 nT (at $R \sim 2.5\, R_E$). Third, the EIC waves propagate predominantly across the magnetic field ($k_\perp \gg k_{||}$); this means that in the structures associated with the EIC waves $E_\perp \gg E_{||}$, at the same frequency, which is not the case for the event under consideration.

In the opposite case, for the observed parallel electric field perturbation there is no significant perturbations of $E_\perp$ at the same spatial/temporal scales, hence $E_{|} \gg E_\perp$ and $k_{||} \gg k_\perp$, as it happens for the ion acoustic wave. In this paper, we argue that the parallel electric field, as well as density variations, are produced by ion acoustic waves excited by primary Alfvén wave. First, we will describe a simple numerical 1-D model which demonstrates the parametric excitation of acoustic waves by Alfvén waves in a single fluid plasma. Finally, we will discuss the possibility of similar excitation of ion acoustic waves in real auroral plasma.

2 Single fluid one-dimensional model

We have performed a simulation of a standing Alfvén wave evolution in a single fluid magnetohydrodynamic (MHD) approximation in one spatial dimension, with three components of **B** and **V** included in the model (i.e. 1.5-D MHD). The normalized 1.5-D MHD equations (e.g. Ofman, 2002) in the ideal limit are:

$$\frac{\partial \rho}{\partial t} + \frac{\partial}{\partial x}(\rho V_x) = 0 \tag{1}$$

$$\rho\left(\frac{\partial \boldsymbol{V}}{\partial t} + V_x \frac{\partial}{\partial x}\boldsymbol{V}\right) = -\nabla p + (\nabla \times \boldsymbol{B}) \times \boldsymbol{B} \tag{2}$$

$$\frac{\partial \boldsymbol{B}}{\partial t} = \nabla \times (\boldsymbol{V} \times \boldsymbol{B}) \,, \tag{3}$$

where only $\partial/\partial x$ terms are included in the curl in Eqs. (1)–(3). In the present model we have used the isothermal energy equation ($T=T_0$=const.), and p is then proportional to ρ. The excitation of the compressional waves occurs through the second term on right-hand side of Eq. (2). The x-component of this quadratically nonlinear term can be written as $-\frac{1}{2}\frac{\partial}{\partial x}B^2$, where $\boldsymbol{B}$ is the transverse magnetic field fluctuation due to the Alfvén wave. Thus, the temporal and the spatial fluctuations of the magnetic pressure produced by the Alfvén wave drive the fluctuations in the parallel (x component) velocity, and consequently in density coupled through the continuity Eq. (1), producing the acoustic waves. This mechanism was found to generate low frequency acoustic waves in the solar wind, in models that include Alfvén waves (e.g. Ofman and Davila, 1998).

The use of a single fluid approximation is justified by the following reasons. Of course, for the single fluid MHD, the true electric field equals zero in the frame of reference moving along with the plasma. However, such a model enables us to follow the development and propagation of the sound wave and to calculate the plasma pressure gradient associated with the wave. On the other hand, according to a two-fluid model, neglecting the electron inertia and gravity, the effective measured electric field is $E^* = E - \frac{\nabla p_e}{ne} \sim \frac{\nabla p_e}{ne}$, i.e. the force acting on electrons is balanced by the electron pressure gradient. In our single fluid model, the ion and electron pressure gradients are equal. Therefore, using the results of the single fluid model, E_x can be estimated as $\frac{1}{2}\frac{\nabla p}{ne} = \frac{T}{2ne}\frac{\partial n}{\partial x}$.

All parameters were assumed to change only along the x-direction in the region $0<x<100$. Unperturbed dimensionless values are chosen as $B_0 \equiv B_x = 1$ for the magnetic field and $\rho_0 = 1$ for the mass density. The pressure $p_0 = 0.1/4\pi$ was chosen in such a way that the speed of sound is ten times smaller that the Alfvén velocity: $c_s = \sqrt{\gamma \frac{p_0}{\rho_0}} = 0.1 V_A = 0.1 \frac{B_0}{\sqrt{4\pi\rho_0}}$. For simplicity, we assume that the adiabatic index $\gamma \equiv 1$ (isothermal process). The Alfvén wave was excited by applying the following boundary condition:

$$B_y(0) = 0.1 B_0 \sin \omega_A t \tag{4}$$

$$B_y(100) = -0.1 B_0 \sin \omega_A t \,, \tag{5}$$

where $\omega_A = \sqrt{\pi}/200$ was chosen in such a way that the Alfvén wavelength λ_A is twice the length of the simulation box. As a result, a standing Alfvén wave arises with a node at $x=0$ and anti-nodes at the boundaries.

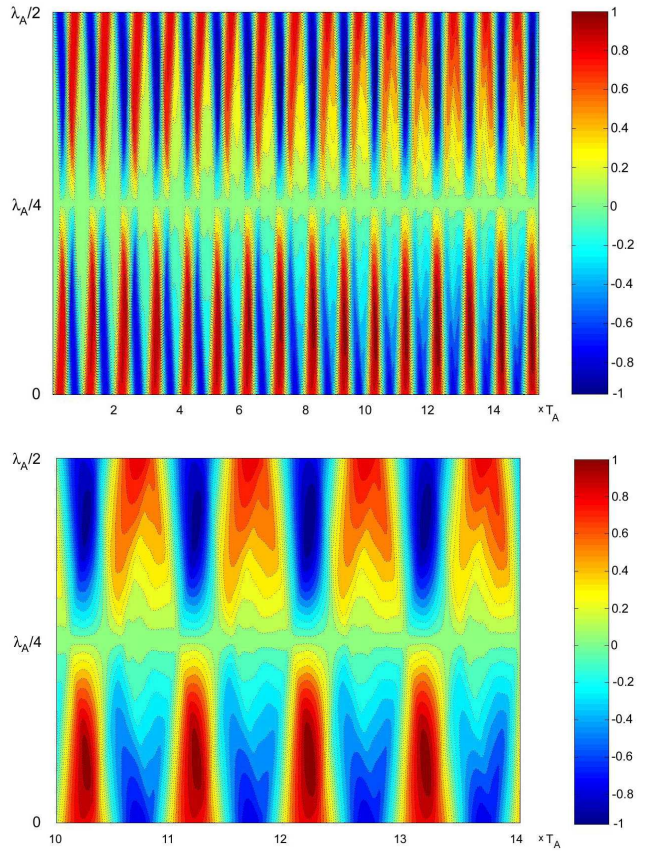

Fig. 2. Spatial and temporal dependence of the magnetic field perturbation B_y. Horizontal axes give the time in T_A units, and vertical axes give the length along the simulation box in λ_A units. Color scale shows the magnitude of B_y. (**a**) Time interval (0–15T_A); (**b**) time interval (10–15T_A).

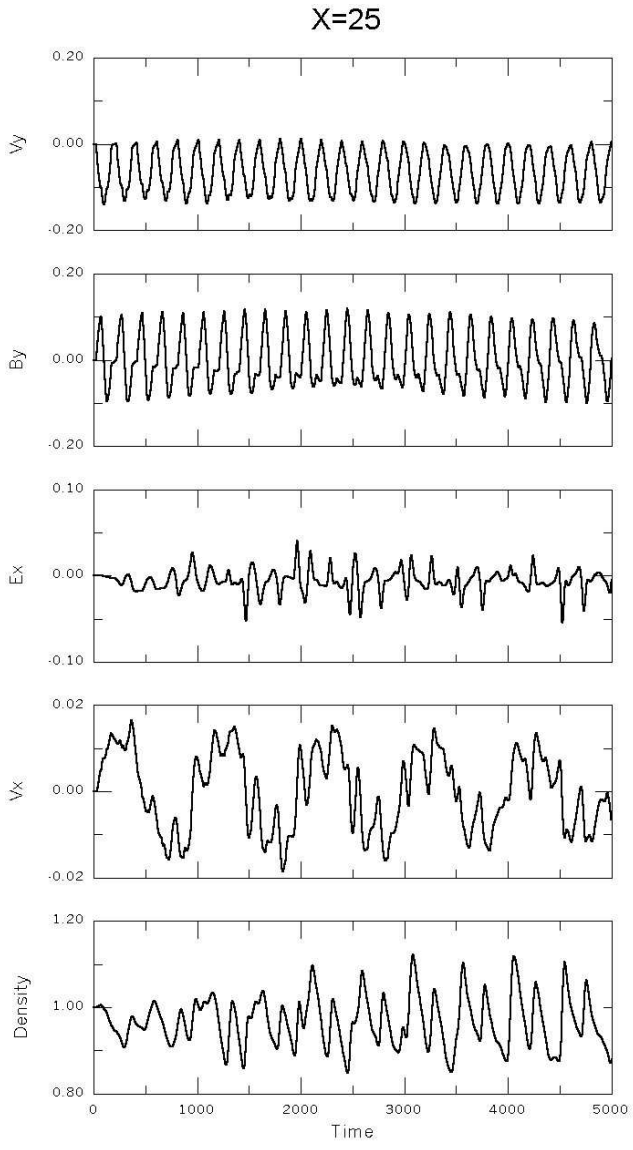

Fig. 3. Time variation of the plasma parameters at the distance x=25 (quarter of the simulation box). From top to bottom: transverse components of the velocity v_y and the magnetic field B_y, parallel electric field E_x and parallel velocity v_x, and the plasma density n.

Additional boundary conditions were:

$$v_x(0) = v_x(100) = 0 \tag{6}$$

$$\frac{\partial\rho(0)}{\partial z} = \frac{\partial\rho(100)}{\partial z} = 0\,. \tag{7}$$

The 1.5-D single fluid MHD equations were solved by the 4th order Runge-Kutta method in time, and 4th order differencing in space (e.g. Ofman, 2002).

Figure 2a shows the time evolution of the $B_y(x)$ component for the time interval t=0–15T_A (here T_A=2π/ω_A is the period of the excited wave). Starting from $t\sim$4T$_A$ the symmetry between positive and negative half-periods is violated indicating the nonlinear evolution of the original wave. This effect is illustrated in figure 2b which shows the $B_y(t,x)$ dependence in increased scale for t=10T$_A$–14 T$_A$.

Figures 3 and 4 give the time dependences (from top to bottom) of v_y, B_y, E_x, v_x, and ρ, for x=25 and x=50, respectively.

One can see that perturbations of parallel velocity and plasma density, which are absent in the linear Alfvén wave, develop in the system. These perturbations are produced by acoustic waves rather than by Alfvén wave nonlinearity. Indeed, let us consider the temporal evolution of spatial spectra of plasma parameters $B_y(k)$, $v_x(k)$, and $\rho(k)$ which are shown in Fig. 5. The spatial spectra of the magnetic field perturbation B_y (Fig. 5a) do not exhibit significant change with time. These spectra possess strong maximum corresponding to the primary wavelength (k$_A$=2π/λ_A=2π/200), and additional small maxima at k=3k_A and k=5k_A. As the nonlinear effects become significant (t>4T$_A$, see Fig. 2a), the spectra become wider and differ significantly for two adjacent half-periods of the original Alfvén waves, but no additional maxima appear. In contrast, dynamical spatial spectra of the parallel electric field (Fig. 5b), starting from $t\sim$5T$_A$, develop new maxima at k=9k_A and k=11k_A corresponding to

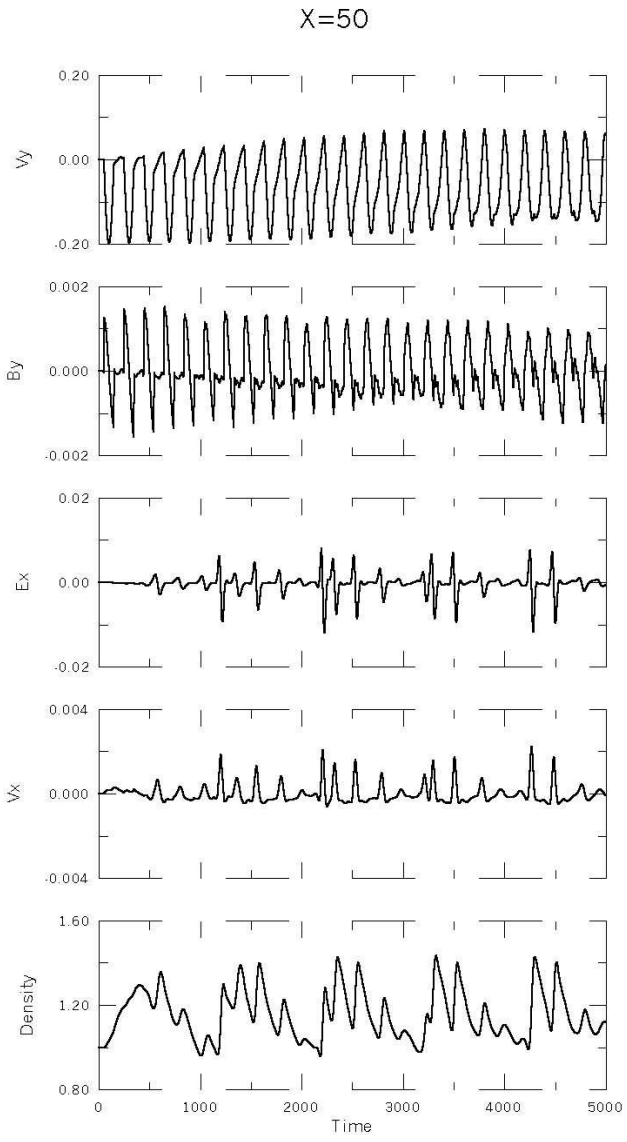

Fig. 4. Same as Fig. 3, but for x=50 (midpoint of the simulation box).

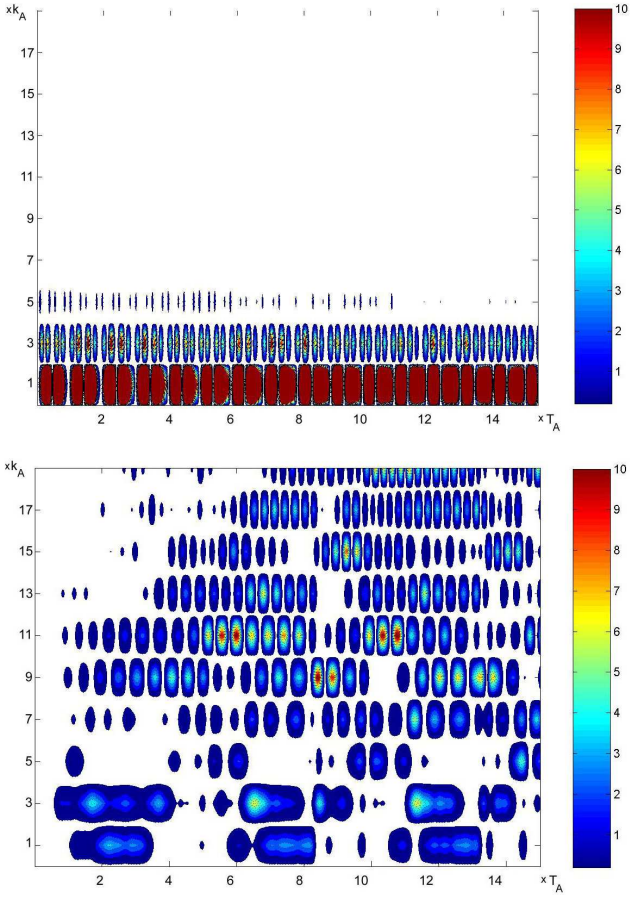

Fig. 5. Time dependence of spatial spectra of the magnetic field perturbation $B_y(t,k)$ (**a**), and the parallel electric field $E_x(t,k)$ (**b**). Horizontal axes give the time in T_A units, and vertical axes give the wave number in k_A units. The values of $B_y(t,k)$ and $E_x(t,k)$ are shown in arbitrary units by color scale.

the wavelength $\lambda\sim 20$. Note that this is the wavelength for the acoustic wave with the frequency ω_A. Later, additional maxima at higher k appear in spatial spectra of the parallel electric field which might indicate the development of acoustic turbulence in the system.

In order to verify whether the perturbations of plasma density, parallel velocity and parallel electric field are produced by acoustic waves rather than by a nonlinear Alfvén wave, we have calculated 2-D Fourier transformations of the simulated variables. The results are shown in Fig. 6. Straight lines show the dispersion relations for Alfvén wave $\omega = V_A k$ and for the acoustic wave $\omega = c_s k$. The 2-D-spectrum $B_y(\omega,\mathrm{k})$ (Fig. 6a) fits well the Alfvén wave dispersion curve. Spatial perturbations with zero frequency are also seen in this spectrum. They result from the distortion of the background due to propagation of the Alfvén wave with finite amplitude.

Two-dimensional spectrum of the parallel electric field $E_x(\omega,\mathrm{k})$ (Fig. 6b) fit perfectly the acoustic wave dispersion curve. Having maximum near ω_A, acoustic waves cover wide range of frequencies.

The mechanism of acoustic wave excitation in this numerical experiment is quite clear. Magnetic pressure perturbation appearing in the nonlinear Alfvén wave produces perturbation of the plasma pressure. The latter possesses the frequency and wavelength of primary Alfvén waves, and can propagate along the magnetic field lines as acoustic waves. The frequencies of acoustic waves are determined by the space/time properties of the plasma pressure perturbation produced by the Alfvén wave. Therefore, the major frequencies are ω_A and $c_s/\lambda_A = \omega_A c_s/V_A$ and their harmonics, the effect of which can be seen in Fig. 6.

3 Discussion

In real ionospheric plasma, the acoustic waves may be excited not only by the magnetic pressure perturbation produced by a nonlinear Alfvén wave. Ion sound instability, as

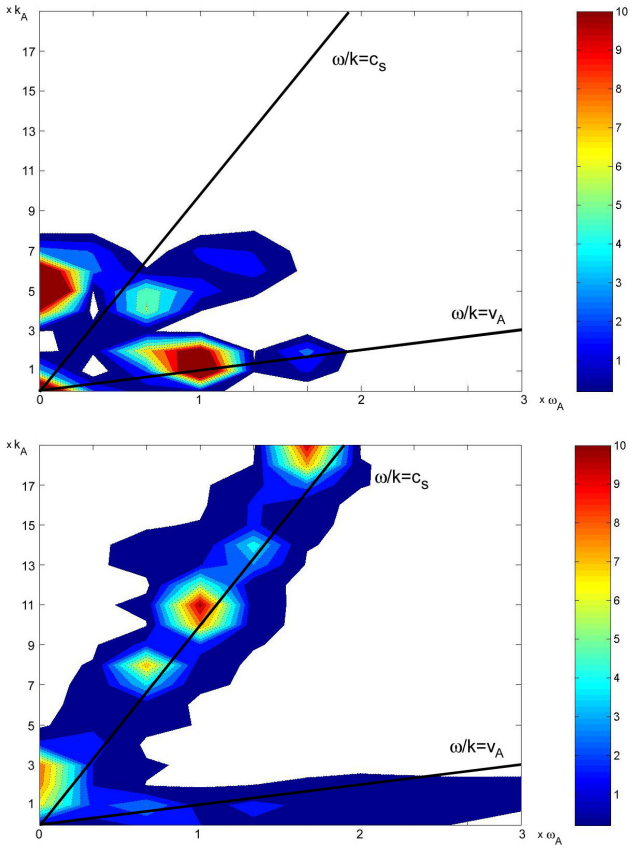

Fig. 6. Two-dimensional spectra of the magnetic field perturbation $B_y(\omega,\mathrm{k})$ and the parallel electric field $E_x(\omega,\mathrm{k})$, calculated for the time interval $10T_A$-$15T_A$. Horizontal axes give the frequency in ω_A units, and vertical axes give the wave number in k_A units. The values of $B_y(\omega,\mathrm{k})$ and $E_x(\omega,\mathrm{k})$ are shown in arbitrary units by color scale. Solid lines denote the dispersion curves for Alfvéng and sound waves.

well, may initiate ion sound waves in the strong electromagnetic auroral perturbations, and can be modeled by two fluid plasma. These perturbations are localized ($k_\perp \gg k_{||}$) standing Alfvén waves, hence, they can also be interpreted as an oscillating localized field-aligned current. It is also known, (e.g. Dubinin et al., 1985, 1986, 1990) that the parallel electric field appears only in especially strong perturbations. We theorize that this occurs when the velocity of current carriers of the field-aligned current exceeds a certain critical value, for example ion sound velocity.

Let the electromagnetic perturbation be the standing Alfvén wave. If the amplitude of the parallel (to the magnetic field) velocity of electrons, v_e, in the wave becomes larger than the ion sound velocity, then during these time intervals the ion sound instability may develop in the plasma. The frequency of these intervals is double the frequency of the initial Alfvén wave. Thus, we obtain a kind of parametric resonance excitation of ion sound waves with the frequency equal to double the frequency of the primary Alfvén wave. This was the case for the observed event shown in Fig. 1. The parallel electric field, E_z, can be estimated as $E_z = \frac{\nabla p_e}{ne} \sim \frac{T_e}{ne}\frac{\partial n}{\partial z}$. If it results from the propagation of ion sound wave $n = n_0 \cos kz$, then the amplitude of the parallel electric field is

$$E_z \sim \frac{T_e}{e}k = \frac{c_s^2 M}{e}\frac{2\pi f}{c_s} = c_s \frac{2\pi f M}{e}\,, \qquad (8)$$

where k is the wave number, f is the frequency of parallel electric field oscillations, c_s is the ion sound velocity, and M is the ion mass (O^+ in our case). If the waves are excited by the ion sound instability, then the phase velocity of the wave equals the velocity of the current carriers and c_s can be estimated as j/ne, where j is the electric current density in the localized electromagnetic perturbation. The latter is given by $j \approx \frac{c}{4\pi}\frac{\Delta B_y}{\Delta x}$, where ΔB_y is the magnetic field perturbation and Δx is the transverse characteristic scale of the perturbation. Substituting ΔB_y=120 nT, $\Delta x = 5\cdot 10^5$ cm, and n=$8\cdot 10^3$ cm^{-3}, one obtains the estimate for the ion sound velocity $c_s \cong 1.4\cdot 10^6 cm/s$.

The sound velocity corresponds to the electron temperature of 30 eV, which seems reasonable for the auroral zone at the altitude of 1000 km. Taking the frequency of the parallel electric field oscillation to be 2 Hz (see Fig. 1), the parallel electric field perturbation is $E_z \cong 28.2 mV/m$ in agreement with the observations.

4 Discussion and conclusion

The existence of upward and downward beams of energetic particles indicates that a drop in the electric potential of the order of several kV occurs along the auroral magnetic field lines. It is clear from observations that the regions of acceleration are rather large, at least larger than $1R_E$. Therefore, the electric field responsible for the field-aligned particle acceleration cannot exceed more than ~2 mV/m. Hence, strong a parallel electric field reaching tens of mV/m is not the direct cause of the acceleration.

There are several ways to explain the appearance of the potential drop along the auroral field lines, for example, by the presence of a parallel component of the electric field in the inertial Alfvén wave. However, the most promising approach is the development of anomalous resistivity. Recently, parallel electric field perturbations (for higher altitudes relevant to Polar satellite) have been modeled by Streltsov et al. (2002). Using nonlinear two-fluid MHD simulations, they have shown that parallel convective nonlinearity (which is in fact due to the electron inertia) does not produce significant a parallel electric field that may be responsible for particle acceleration into the ionosphere, whereas the relevant values of the parallel electric field can be explained by the presence of anomalous resistivity (AR). However, the AR was not included self-consistently in their model; instead, the effective collisional frequency was adopted from the model by Lysak and Dum (1983) for EIC instability. Therefore, the spatial/temporal scales for $E_{||}$ in their model are the same as for $E_\perp$. This is quite natural, since self-consistent consideration of the effects of anomalous resistivity requires kinetic simulation.

In fact, the local electric field measurements by satellites refer to the field of the waves responsible for the AR rather than to the "global accelerating" field. This is the reason why the observed parallel electric field is so strong – the wavelengths producing the AR are small, and the parallel potential drops due to these waves are of the order of tens of volts. These small drops only modulate the accelerated beam on a global scale, as can be seen in the two lower panels of Fig. 1. As we discussed above, the structure of the electrostatic wave producing strong parallel electric field (at least at the altitudes $\sim$1000 km) is similar to the ion acoustic rather than the EIC wave. Acoustic waves are excited in the plasma as a result of the propagation of the Alfvén wave with finite amplitude and account for the parallel electric field observed in the small-scale electromagnetic perturbations of auroral plasma. This effect is modeled by a single fluid MHD model. In our simulation, the magnetic pressure perturbation appearing in the nonlinear Alfvén wave produces perturbation of the plasma pressure with the same frequency ω_A and wavelength λ_A as those of the primary Alfvén wave. The plasma pressure perturbation propagates as an acoustic wave. Therefore, new frequencies $\sim\lambda_A/c_s$ and wavelengths $\sim c_s/\omega_A$ arise in the spectrum of secondary acoustic waves. The excitation of acoustic modes is extremely effective if the parallel electric current associated with the localized standing Alfvén waves is so strong that the velocity of current carriers exceeds the threshold of the ion sound instability.

Acknowledgements. PLI would like to acknowledge support by the Binational Science Foundation (BSF) grant. LO would like to thank the Department of Geophysics for the hospitality during his visits at Tel Aviv University, and acknowledge support by NASA Sun-Earth Connection Theory program, and NASA grant NAG5-11877.

Topical Editor M. Lester thanks a referee for his help in evaluating this paper.

References

Andre, M., Koskinen, H., Gustafsson, G., and Lundin, R.: Ion waves and upgoing ion beams observed by the Viking satellite. Geophys. Res. Lett., 14, 463–466, 1987.

Bennett, E. L., Temerin, M. and Mozer, F. S.: The distribution of auroral electrostatic shocks below 8000 km altitude, J. Geophys. Res. 88, 7107–7120, 1983.

Burke, W. J., Silevitch, M. and Hardy, D. A.: Observations of small scale auroral vortices by S3-2 satellite,J. Geophys. Res. 88, 3127–3137, 1983.

Cattell, C. A., Kim, M., Lin, R. P., and Mozer, F. S.: Observations of large electric fields near the plasma sheet boundary by ISEE-1, Geophys. Res. Lett., 9, 539–542, 1982.

Cattell, C. A., Mozer, F. S., Tsuruda, K., Hayakawa, H., Nakamura, M., Okada, T., Kokubun, S., and Yamamoto, T.: Geotail observations of spiky electric fields and low-frequency waves in the plasma sheet and plasma sheet boundary, Geophys. Res. Lett., 21, 2987–2990, 1994.

Cattell, C., Bergmann, R., Sigsbee, K., Carlson, C., Chaston, C., Ergun, R., McFadden, J., Mozer, F. S., Temerin, M., Strangeway, R., Elphic, R., Kistler, L., Moebius, E., Tang, L., Klumpar, D., and Pfaff, R.: The association of electrostatic ion cycltron waves, ion and electron beams, and field-aligned currents: FAST observations of an auroral zone crossing near midnight, Geophys. Res. Lett., 12, 2053–2056, 1998.

Dubinin, E. M., Podgorny, I. M., Balebanov, V. M., Bankov, L., Bochev, A., Gdalevich, G. L., Dachev, Tz., Zhuzgov, L. N., Kutiev, I., Lazarev, V. I., Nikolaeva, N. S., Serafimov, K., Stanev, G. and Teodosiev, D.: Intense localized disturbances of the auroral ionosphere, Kosmicheskiye Issledovaniya, 22, 247–254, 1984.

Dubinin, E. M., Israelevich, P. L., Kutiev, I., Nikolaeva, N. S. and Podgorny, I. M.: Localized auroral disturbance in the morning sector of topside ionosphere as a standing electromagnetic wave, Planet. Space Sci. 33, 597–606, 1985.

Dubinin, E. M., Israelevich, P. L., Nikolaeva, N. S., Podgorny, I. M., Bankov, N. and Todorieva, L.: The electromagnetic structures at the auroral altitudes, Kosmicheskie Issledovaniia 24, 434–439, 1986.

Dubinin, E. M., Israelevich, P. L., and Nikolaeva, N. S.: Auroral electromagnetic disturbances at an altitude of 900 km: The relationship between the electric and magnetic field variations, Planetary Space Science, 38, 97–108, 1990.

Gelpi, C. G. and Bering, E. A.: The plasma wave environment of an auroral arc—2. ULF-waves on an auroral arc boundary, J. Geophys. Res. 89, 10 847–10 864, 1984.

Glassmeier, K.-H., Lester, M., Mier-Jedrzejowicz, W. A. C., Green, C. A., Rostoker, G., Orr, D., Wedeken, U., Junginger, H., and Amata, E.: Pc5 pulsations and their possible source mechanisms: a case study, J. Geophys., 55, 108–119, 1984.

Goertz, C. K., (1984), Kinetic Alfvén waves on auroral field lines, Planetary Space Sci, 32, 1382–1387, 1984.

Goertz, C. K. and Boswell, R. W.: Magnetospheric-ionospheric coupling. J. Geophys. Res., 84, 7239–7246, 1979.

Gurnett, D. A., Huff, R. L., Menietti, J. D., Winningham, J. D., Burch, J. L. and Shawhan, S. D.: Correlated low-frequency electric and magnetic noise along the auroral field lines, J. Geophys. Res., 89, 8971–8985, 1984.

Haerendel, G.: An Alfvén wave mode of auroral arcs, in: High Latitude Space Plasma Physics, edited by Hultquist, B. and Hagfors, T., Plenum Publishing Corporation, New York, 515–535, 1983.

Hasegawa, A.: Particle acceleration by MHD surface wave and formation of aurora, J. Geophys. Res., 81, 5083–5089, 1976.

Karlsson, T., and Marklund, G. T.: A statistical study of intense low-altitude electric fields observed by Freja, Geophys. Res. Lett., 23, 1005–1008, 1996.

Kindel, J. M. and Kennel, C. F.: Topside current instabilities, J. Geophys. Res., 76, 3055–3078, 1971.

Kintner, P. M.: On the distinction between electrostatic ion cyclotron wave and ion cyclotron harmonic waves, Geophys. Res. Lett., 8, 585–588, 1980.

Levin, S., Whitley, K., and Mozer, F. S.: A statistical study of large electric field events in the Earth's magnetotail, J. Geophys. Res., 88, 7765–7768, 1983.

Lindqvist, P.-A. and Marklund, G. T.: A statistical study of high-altitude electric fields measured on the Viking satellite, J. Geophys. Res., 95, 5867–5876, 1990.

Lysak, R. L. and Carlson, C. W.: Effect of microscopic turbulence on magnetosphere-ionosphere coupling. Geophys. Res. Lett., 8, 269–272, 1981.

Lysak, R. L. and Dum, C. T.: Dynamics of magnetosphere-ionosphere coupling including turbulent transport. J. Geophys. Res., 88, 365–380, 1983.

McIlwain, C. E.: Direct measurement of particles producing visible auroras, J. Geophys. Res., 65, 2727–2749, 1960.

Mallinckrodt, A. J. and Carlson, C. W.: Relations between transverse electric fields and field-aligned currents. J. Geophys. Res. 83, 1426–1432, 1978.

Mishin E. V., Burke, W. J., Huang, C. Y., and Rich, F. J.: Electromagnetic wave structures within subauroral polarization streams, J. Geophys. Res., 108, A8, 1309, doi:10.1029/2002JA009793, 2003.

Mizera, P. F., Fennell, J. F., Croley, D. R., Vampola, A. L., Mozer, F. S., Torbert, R. B., Temerin, M., Lysak, R., Hudson, M., Cattell, C., Johnson, R. J., Sharp, R. D., Ghielmetti, A. G. and Kinter, P. M.: The aurora inferred from S3-3 particles and fields. J. Geophys. Res., 86, 2329–2339, 1981.

Mozer, F. S.: ISEE-1 observations of electrostatic shocks on auroral zone field lines between 2.5 and 7 Earth radii, Geophys. Res. Lett., 8, 823–826, 1981.

Mozer, F. S., Carlson, C. W., Hudson, M. K., et al.: Observations of paired electrostatic shocks in the polar magnetosphere, Phys. Rev Lett., 38, 292–295, 1977.

Mozer, F. S., Cattell, C. A., Hudson, M. K., Lysak, R. L. Temerein, M. and Torbert, R. B.: Satellite measurements and theories of low altitude auroral particle acceleration, Space Sci. Rev. 11, 155–213, 1980.

Ofman, L.: Chromospheric leakage of Alfvén waves in coronal loops, Ap. J., 568, L135–L138, 2002.

Ofman, L. and Davila, J. M.: Solar Wind Acceleration by Large-amplitude Nonlinear Waves: Parametric study, J. Geophys. Res., 103, 23 677–23 690, 1998.

Pokhotelov O. A., Onishchenko, O. G., Sagdeev, R. Z., and Treumann, R. A.: Nonlinear dynamics of inertial Alfvén waves in the upper ionosphere: Parametric generation of electrostatic convective cells, J. Geophys. Res., 108, 1291, doi:10.1029/2003JA009888, 2003.

Redsun, M. S., Temerin, M., and Mozer, F. S.: Classification of auroral electrostatic shocks by their ion and electron associations, J. Geophys. Res., 90, 9615–9633, 1985.

Shelley, E. G., Sharp. R. D., and Johnson, R. G.: Satellite observations of an ionospheric acceleration mechanism, Geophys. Res. Lett., 3, 654–656, 1976.

Streed, T, C., Cattell, F., Mozer, S., Kokubun, and Tsuruda, K.: Spiky electric fields in the magnetotail, J. Geophys. Res., 106, 6276–6289, 2001.

Streltsov, A. V. and Lotko, W.: Small-scale electric fields in downward auroral current channels, J. Geophys. Res., 108, A7, 1289, doi: 10.1029/2003JA009858, 2003.

Streltsov, A. V. and Mishin, E. V.: Numerical modeling of localized electromagnetic waves in the nightside subauroral zone, J. Geophys. Res., 108, A8, 1332, doi:10.1029/2003JA009858, 2003.

Streltsov, A. V., Lotko, W., Keiling, A., and Wygant, J. R.: Numerical modeling of Alfvén waves observed by the Polar spacecraft in the nightside plasma sheet boundary layer, J. Geophys. Res., 107, A8, doi:10.1029/2001JA000233, 2002.

Temerin, M., Cattell, C. A., Lysak, R., Hudson, M., Torbert, R. B., Mozer, F. S., Sharp, R. D. and Kintner, P. N.: The small scale structure of electrostatic shocks, J. Geophys. Res. 86, 11 278–11 298, 1981.

Volokitin, A. S., Krasnoselskikh, V. V., Mishin, Ye. V., Tyurmina, L. O., Sharova, V. A. and Shkolnikova, S. I.: On the small scale structure of field aligned currents at high latitudes. Preprint IZMIRAN, N 18 (429), 1983.

Weimer, D. R. and Gurnett, D. A.: Large-amplitude auroral electric fields measured with DE 1, J. Geophys. Res., 98, 13 557–13 564, 1993.

Wygant, J. R., Keiling, A., Cattell, C. A., et al.: Polar spacecraft based comparison of intense electric fields and Poynting flux near and within the plasma sheet-tail lobe boundary to UVI images: An energy source for the Aurora, J. Geophys. Res., 105, 18 675–18 692, 2000.